Influence of Rising Sea Level on Tidal Dynamics in the Bohai Sea

Authors: Li, Yanfang, Zhang, Hua, Tang, Cheng, Zou, Tao, and Jiang, Dejuan

Source: Journal of Coastal Research, 74(sp1) : 22-31

Published By: Coastal Education and Research Foundation

URL: https://doi.org/10.2112/SI74-003.1

Journal of Coastal Research	SI	74	22–31	Coconut Creek, Florida	2016

Influence of Rising Sea Level on Tidal Dynamics in the Bohai Sea

Yanfang Li[‡*], Hua Zhang[‡], Cheng Tang[‡], Tao Zou[‡], and Dejuan Jiang[‡]

[‡] Key Laboratory of Coastal Environmental Processes and Ecological Remediation
Yantai Institute of Coastal Zone Research
Chinese Academy of Sciences
Yantai, Shandong 264003, P. R. China

www. cerf-jcr. org

www. JCRonline. org

ABSTRACT

Li, Y. F.; Zhang, H.; Tang, C.; Zou, T., and Jiang, D. J., 2016. Influence of rising sea level on tidal dynamics in the Bohai Sea. *In*: Harff, J. and Zhang, H. (eds.), *Environmental Processes and the Natural and Anthropogenic Forcing in the Bohai Sea, Eastern Asia. Journal of Coastal Research*, Special Issue, No. 74, pp. 22–31. Coconut Creek (Florida), ISSN 0749-0208.

Recent studies highlight that tidal propagation in shallow waters tends to be modified with mean sea level rise, intensifying coastal threats. This study aims to obtain a comprehensive insight into the changes in tidal regimes in the Bohai Sea of China in response to local mean sea level rise. To achieve this goal the hydrodynamic model ROMS, previously calibrated and validated for Bohai Sea, was applied, considering local sea level rise scenario of 0. 5 m, 1 m, 2 m and 3 m in the future, respectively. The model results show that under sea level rise conditions the amplitude of the main semidiurnal (M_2) constituent decreases in most areas except two areas where are around two amphidromic points, and changes in amplitude are not proportional to the level of sea level rise. However, compared results implied that it is necessary to consider the spatial-distribution of sea level-rise when predicting the effects of sea level rise in the future. The tidal wave also was distorted in the coastal zone, the changed wavelength made the amphidromic points move to deep water. Tidal current magnitude decreases with mean sea level rise, which could influence transport of sediment nearby coast of Bohai and Laizhou Bay.

ADDITIONAL INDEX WORDS: *Sea level rise, amplitude, amphidromic point, tidal current, spatial distribution.*

INTRODUCTION

The Bohai Sea is a semi-enclosed sea with shallow water (Figure 1a), which average water depth is only 18 m, surrounded by cities in the north Chinese Sea. In the Bohai Sea barotropic tides are the dominant circulation processes, having considerable amplitudes as well as momentum and energy fluxes. Because of the effects of enhanced bottom friction associated with shallow shelf topography, tides and tidal residual currents play an important role in affecting many other physical and biogeochemical processes in this region (Wei *et al.*, 2003).

Accelerated economic development and large land reclamation have changed the coastline along the Bohai Sea. In the western Bohai Bay the large land reclamation of about 129. 7 km^2 (SOAPRC, 2009), and to the northeast of Laizou Bay an artificial island of 35. 2 km^2 was built, which both reconstructed the coastline. Since the shift of the Yellow River mouth has influenced the amphidromic points of M_2 to move (Wang *et al.*, 2014), Huang *et al.* (2015) evaluated the influence of coastline modification in the Bohai Sea based on four different coastlines of 2000, 2008, 2010, and 2012, and found that the changed coastlines could move the amphidromic point and modify tide amplitudes, especially making the amphidromic point near the Yellow River estuary move towards south-east. Therefore it is important to use the newest coastline and accurate topography for tide models in the Bohai Sea.

It is an irrefutable fact that global warming causes sea level to rise. Accelerated sea level rise (SLR) can drastically affect coastal regions, such as submerging and increased flooding of lower-land. Except for these direct effect of increased high water level, on longer term scale SLR could influence tidal system (Pelling *et al.*, 2013a; 2013b; Pickering *et al.*, 2012; Zhang *et al.*, 2013). The basic physical consequence to such changes is the variation in tidal dynamics (Chu-Agor *et al.*, 2011; Muller *et al.*, 2011; Pickering *et al.*, 2012; Poulos *et al.*, 2009; Snoussi *et al.*, 2009; Ward *et al.*, 2012). Some studies have shown that SLR has a direct effect on coastal tides. On the European shelf Pickering *et al.* (2012) found that tidal response of M_2 is non-linear to future SLR with spatial variation in amplitude. Ward *et al.* (2012) studied the different effects of the way of SLR implemented in the model, flooding could intensify the response caused by SLR (Pelling and Green, 2013), the main difference of tidal response was found in the Bohai Bay and Liaodong Bay between flood and no-flood, but very small difference between flood and partial-flood (Pelling *et al.*, 2013b). Gong *et al.* (2012) studied the effects of sea level rise on Yangtze estuary and found that tidal wave changed slightly in nearshore areas. Zhang *et al.* (2013) studied the tidal system changes due to sea level rise in China, and found that the enhanced amplitude was in the north to amphidromic point, while phase lags were increased to the

DOI: 10. 2112/SI74-003. 1 received (8 January 2015); accepted in revision (1 June 2015).

*Corresponding author: yfli@ yic. ac. cn

eastern. The residual currents could be reduced by 20% caused by SLR change in narrow and shallow channels in Portuguese (Valentim *et al*., 2013). As a major forcing agent SLR could present a substantial influence on coastal erosion worldwide (Cooper and Pilkey, 2004; FitzGerald *et al*., 2008; Leatherman *et al*., 2000). To the Yellow River Delta tidal current was one of main factors causing coastal erosion (Ji and Jiang, 1994). All the results showed that future SLR has significant impacts on the tidal amplitudes, currents and associated tidal dissipation.

There have been many results about tide modeling in Chinese Sea (Bao *et al*., 2001; Fang *et al*., 2004; Kang *et al*., 2002; Lefèvre *et al*., 2000; Song *et al*., 2013; Wang *et al*., 2014; Yao *et al*., 2012; Yu *et al*., 2003). Some Chinese scientists have studied the effects of SLR on Chinese Sea (Kuang *et al*., 2014; Yu *et al*., 2003, 2007), but the conclusions were not consistent, especially the changes of tidal range and phase lags in local Bohai Sea. The influences of SLR on tides depend on local sea level rise and particular coast morphology. In the Bohai Sea from 1993 to 2012 the average satellite altimetry data show that mean sea level had a rising rate of about 3.8 mm/yr in the Bohai Sea, much faster than global average (Church and White, 2006) in Figure 1b. All these conclusions about effects of SLR on coastal tides are most based on a uniform value of SLR, however, there are few studies considering the spatial distribution difference of SLR. To evaluate the potential influence accurately caused by future sea level rise, in this study we use a hydrodynamic model to simulate the tide in Bohai Sea with newest coastline, and according the present sea level rising rate to assess the influence of SLR on tides and residual currents in the Bohai Sea in the future of one hundred years.

This paper is organized as follows: model configuration is described in detail in Section 2, and model results are shown in Section 3, and then followed a discussion and conclusion.

MODEL AND METHODS

Numerical model and set-up

Tides were predicted using the Regional Ocean Modeling System (ROMS) which is a three-dimensional, free-surface, finite difference nonlinear hydrodynamic model, and formulated in a vertical terrain-following sigma coordinate, which was developed by Rutgers and UCLA Universities, USA (Haidvogel *et al*., 2000; Warner *et al*., 2008). The model encompassed the whole Bohai Sea from 37°N to 41.05°N meridionally and from 117.5°E to 122.5°E zonally with a grid resolution of 2′ (about 3 km). Bathymetric data for the model was obtained from a combination of 4 digital nautical charts of different scale around this area, which was provided by Navigation Guarantee Department of the Chinese Navy in 2012 (Figure 1a). The depths were raised by an average tidal range of 1.5 m to convert the low-tide datum into a mean sea level, based on the reference mean sea level value provided in each marine chart. The model has one east-open boundary along which the phases and amplitudes of elevation of main astronomical tidal constituents (M_2, S_2, K_1, O_1) were prescribed. The four major tide constituents forcing were derived from the regional ocean model NAO.99b with 5′ resolution (Matsumoto *et al*., 2000). In the Bohai Sea, with shallow water tidal models are sensitive to bottom friction coefficient, and according to former simulations (Lu and Zhang, 2006; Pelling *et al*., 2013a; Song *et al*., 2013; Yao *et al*., 2012), the drag coefficient in the model was tuned to 1.2×10^{-3} m/s to minimize the simulation errors.

The simulations were set up to enable inter-comparison and therefore all parameters were kept constant with the exception of sea level rise. The first standard experiment represents the present state (case 0), then we run four cases with different value of uniform SLR in the Bohai Sea to access the sensitivity and linearity of tidal response with respect to SLR, the runs indexed with the number 0.5, 1, 2, 3 to represent the increment of SLR scenarios in meter, respectively, and another experiment indexed with '100y' means that spatial-distribution values after the current non-uniform SLR rate lasting for one hundred years.

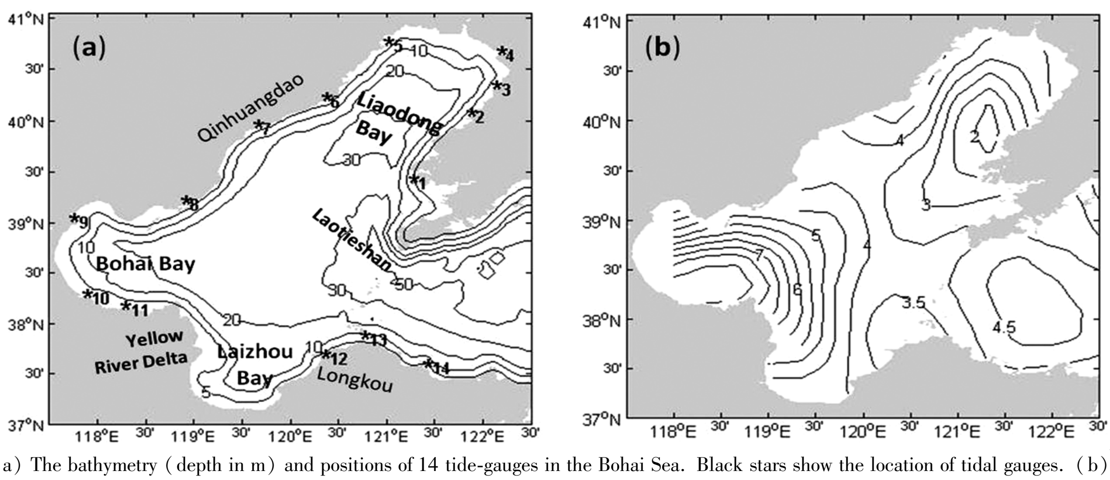

Figure 1. (a) The bathymetry (depth in m) and positions of 14 tide-gauges in the Bohai Sea. Black stars show the location of tidal gauges. (b) The distribution of sea level rising trend (mm/yr) during 1993–2012 in the Bohai Sea

Since 2011 the altimeter processing upgraded with the improved corrections, there is no adjustment to agree with tide gauge data (Church and White, 2011; Fu and Cazenave, 2001), the processes of sea level variation obtained with TOPEX/Poseidon altimeter and tide gauge data had a remarkably good agreement (Feng *et al*., 2013; Hu *et al*., 2014), therefore we used the values calculated from satellite altimeter data (The altimeter products were produced by Ssalto/*Duacs* and distributed by *Aviso*, with support from *Cnes*, http://www.aviso.altimetry.fr/duacs/) to represent spatial-distribution of local sea level rise.

All the simulations use the same start date of the 21th of April 2012, to ensure consistent astronomic forcing. This date was chosen because of the quality of the validation data available for this period. The model was spun up over 10 days and the last 30 days was used for harmonic analysis and to coincide with the period of tidal gauge. The co-tidal charts produced were used both for validation and to evaluate the change in tidal constituents by plotting the difference between those co-amplitude fields.

Tidal energy flux and dissipation

The tidal energy flux was calculated according to (Greenberg 1979):

$$F = \frac{\rho_0}{T}\int_0^T (h + \eta) \cdot [1/2 \times (u^2 + v^2) + g\eta] \cdot (u + iv) \times \mathrm{d}t \quad (1)$$

where ρ_0 is the density of seawater, taken as 1,026 kg/m^3, h is the local depth in meters, η is the sea level fluctuations due to tides, u, v are the depth-averaged tidal currents components from the ROMS solutions and g is the gravitational acceleration, 9.8m/s^2. The integration is averaged over M_2 tidal period T (i.e., 12.42 h).

Mathematically, the tidal energy dissipation can be calculated following the scheme proposed by (Munk, 1997; Taylor, 1919):

$$D = \frac{1}{T}\int_0^T C_d \rho_0 (u^2 + v^2)^{\frac{3}{2}} \mathrm{d}t \quad (2)$$

Where C_d is the bottom friction coefficient taken as 0.0012 in our case, the other variables are the same as the above mentioned formula (1) for tidal energy flux. This formula is based on the quadratic bottom stress scheme, which is consistent with our ROMS model configurations.

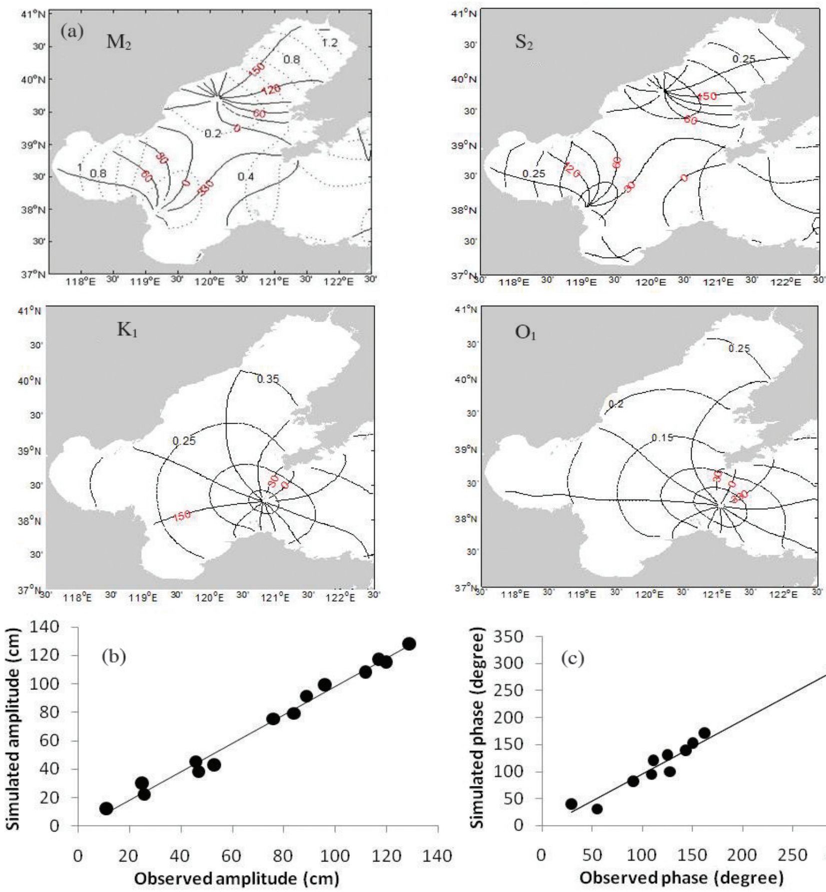

Figure 2. Simulation verification. (a): Cotidal-chart of four main constituents (M_2, S_2, K_1, O_1), dashed line is for amplitude in meter, solid line is phase lag in degree; (b): Comparison between simulated and observed amplitude of M_2; (c): Comparison of phase of M_2

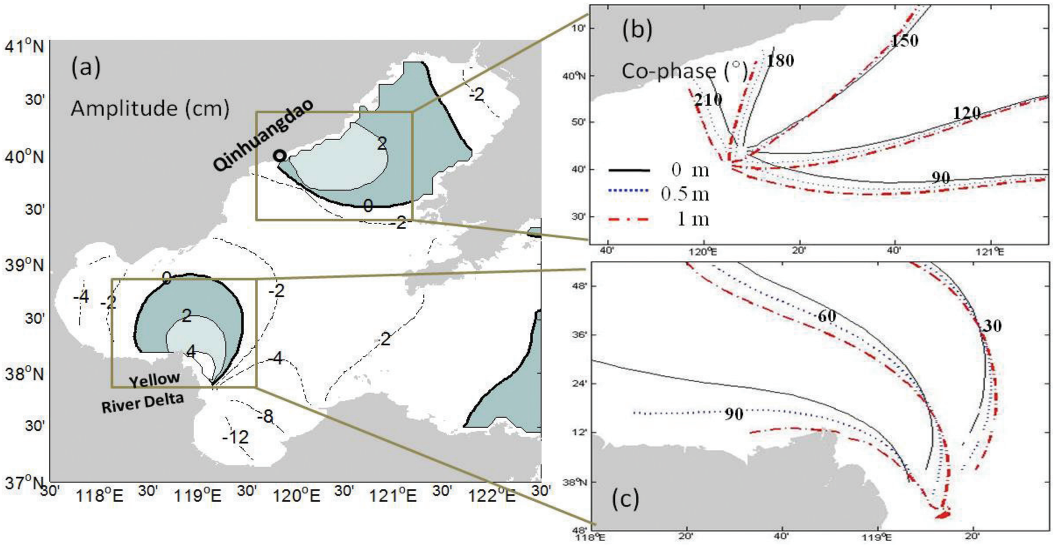

Figure 3. (a) Changes of amplitude of M_2 with SLR 1 meter (unit, cm), the shaded area are where amplitude increases. (b) Shift of co-phase lines near Qinhuangdao Island (black circle) due to different value of SLR and (c) changes near Yellow River Delta (unit: degree), black solid line is the present state, dashed line is SLR 0.5 m, and dot-line is SLR 1 m

Model validation

The basic validation was performed to ensure the model was correctly reproducing the observed tide. There were 14 sets of tidal harmonics for validation derived from tidal gauge and published scientific journals (Chen *et al.*, 2011; Li *et al.*, 2011; Wang *et al.*, 2014; Yao *et al.*, 2012; Figure 1a). Because semidiurnal signal predominated in most parts of the Bohai Sea, we only showed the validation of M_2. Figure 2 showed the accuracy of our simulation. There were two amphidromic points located in Bohai Sea (Figure 2a): one at the offshore area of Qinhuangdao and one near the mouth of the Yellow River, which agreed well with previous publications (Bao *et al.*, 2001; Fang *et al.*, 2004; Yu *et al.*, 2003), and with the new coastline, the changes of Yellow River Delta influenced its surrounding tidal wave and obstructed tidal energy here (Pelling *et al.*, 2013a), the amphidromic point near Old Yellow River Mouth has moved to southeast (Hao *et al.*, 2010). Figure 2b and 2c showed the linear-fit between simulations and observed amplitude and phase lag, respectively, and compared to previous studies (Bao *et al.*, 2001; Song *et al.*, 2013; Zhu and Liu, 2012) the average absolute error of amplitude in this paper is 3.6 cm, and phase error is 7.2°, we also used the variance $VC = 1 - (\frac{R_m}{R_o})^2$ to quantify the model results, where R_o is the root mean squared of observed values and R_m is the root mean squared difference between model and observations (Pelling *et al.*, 2013b). The modeled M_2 amplitudes and phases both achieved a variance captured of 99.4%, which indicated that the errors are well controlled in the whole region, in general the established model of Bohai Sea could capture the tide correctly.

RESULTS

Changes of amplitude and phase

Figure 3 showed the responses of M_2 amplitude and phase to 1 m SLR. When the depth of Bohai Sea increased 1 meter, there exits certain distribution patterns in the differences between the amplitude and phase with different increment of sea level. Figure 3a displays obvious distribution in amplitude change of M_2, there are two areas where amplitude increases (shaded area), one is near the Yellow River Delta and the other in the Liaodong Bay, and the maximum increment of amplitude reached up to 5.5 cm. In the central Bohai basin, Laizhou Bay, Bohai Bay, and northeast of Liaodong Bay, SLR caused amplitude of M_2 to decrease, and the maximum decrement of 12cm appeared in the Laizhou Bay. The spatial distribution pattern of changed amplitude was similar to the result of Pelling *et al.* (2013b) with 2m SLR. However, compared to maximum decrement of 10 cm based on 2m SLR (Pelling *et al.*, 2013b), the discrepancy was mainly caused by flooding. Flooding along the coast could increase energy dissipation, weaken the propagation of reflected tidal wave. The changes of M_2 phase showed a notable distribution. There are some regulations in changes of co-phases, it seems that on the western part near Qinhuangdao (site 7, marked in Figure 1a), co-tidal phase decreased anti-clockwise, while on the right phase lag increased clockwise (Figure 3b); and the same situation appeared in the Yellow River Delta, which was in most agreement with the theoretical model results (Yu *et al.*, 2003), but inconsistent with previous conclusions (Yu *et al.*, 2007), which showed that co-tidal phase changed in a same anti-clockwise direction.

Obviously SLR has changed the characteristics of tide, it can also influence the amphidromic point positions of tidal waves shift relatively to those of current tidal waves. In the shallow water, tidal wave propagated more quickly and wavelength increased with SLR increase, which would shift the amphidromic points. Table 1 showed the movements of amphidromic points under different SLR conditions. It was clear to see the migration of two amphidromic points, one amphidromic point near Yellow River Mouth moved to southeast due to SLR (Yao *et al*., 2012; Yu *et al*., 2007), and the other near Qinhuangdao moved to southwest (also shown in Figure 3b), which would change tidal phase lag.

Change of tidal energy

According to formula (1) we calculated the tidal energy flux distribution in Bohai Sea in different SLR scenario. The simulated current state (no SLR) of M_2 tidal energy flux (Figure 4a) reached a good agreement with results from Song *et al*. (2013) and Yao *et al*. (2012). The tidal energy flux came into the Bohai Sea along the 50 m isobaths through the Bohai Strait, which broke into two branches: one branch turns northward into the Liaodong Bay and the remaining moves westward into the Bohai Sea interior (Zhu and Liu, 2012). And in the Bohai Sea, the maximum tidal energy appeared in the Laotieshan Channel, less than 5 GW, far less than that of Yellow Sea (Yao *et al*., 2012). The mean tidal energy dissipation was also calculated using formula (2) and analyzed to study the changes of tidal energy dissipation in different SLR scenario. The spatial pattern of mean tidal energy dissipation of control run (0 m SLR) was also consistent with previous studies of tidal energy (Kang *et al*., 2002; Song *et al*., 2013; Yao *et al*., 2012), with the largest energy dissipation occurred near coast, especially where coastline was irregular (not shown). Specifically, three sections were chosen to evaluate the effects of SLR on tidal energy (Figure 4b), it was clear to see that with SLR tidal energy entered into the Bohai Sea was decreased by increased energy dissipation, the tidal energy that entered into the Bohai Bay and Laizhou Bay also decreased. At the same condition of SLR increment, tidal energy through the Strait decreased more than those entering into the bays, which implied that with the propagation of tidal wave, the SLR effects on tidal energy decreased gradually.

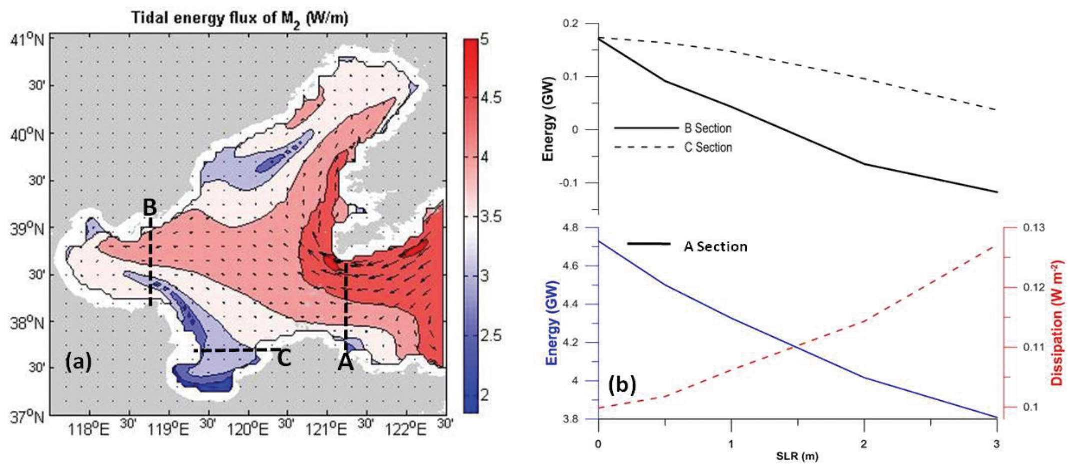

Figure 4. (a) Tidal energy flux of M_2 and energy flux vectors are plotted every three grid points (unit: W m^{-1}, shown as logarithmic values base on 10). (b) Changes of tidal energy in three sections with different SLR, the positive values are energy flowing into Bohai Sea (blue solid line) or Bohai Bay (solid line) and Laizhou Bay (dashed line) with unit of GW, and tidal energy dissipation rate in A section (red dashed line, unit: W/m^2)

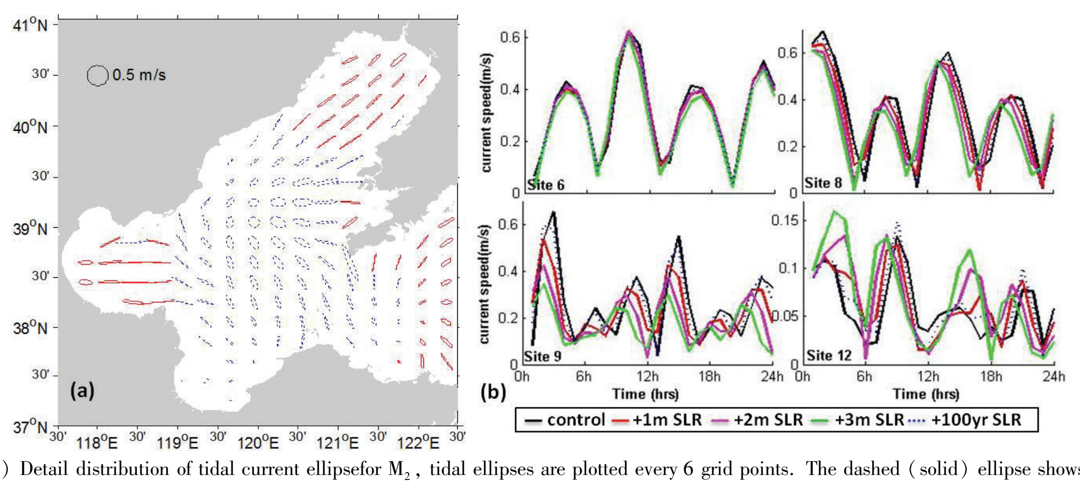

Figure 5. (a) Detail distribution of tidal current ellipsefor M_2, tidal ellipses are plotted every 6 grid points. The dashed (solid) ellipse shows the tidal ellipses rotate clockwise (counter-clockwise). (b) Tidal speed curves (m/s) from different SLR scenario at 4 ports. The five sea level scenarios are shown 0 m (black line), 1 m (red line), 2 m (mauve line), 3 m (green line), and 100 years (blue dashed line). Note that the ports are marked in Figure 1a

Change of tidal current

The characteristics of tidal currents can be depicted by the depth-averaged tidal current ellipses (Figure 5a). In the Bohai Sea, the strongest tidal currents are seen in the Bohai Bay with a maximum speed of about 0.6 m s^{-1} in west-east reversing flow. The weakest current occurs in the Laizhou Bay with a speed of only 0.1 ~ 0.2 m s^{-1}. The tidal currents in the center of Bohai Sea and Laizhou Bay behave as clockwise rotating currents rather than reversing ones appeared in Liaodong and Bohai Bays. And the tidal residual current has been recognized to play an important role influencing long-term sediment and other materials transport (Li *et al.*, 2005; Wei *et al.*, 2004). The mean residual currents in the interior of Bohai Sea are rather small, only of the order of a few cm s^{-1}, and larger residual currents appeared near coast, no more than 5 cm s^{-1}. In the Bohai Bay there was a weak, cyclonic gyre, and there was an anticyclone gyre southwest to Liaodong Peninsula, in the Bohai Strait, the mean tidal residual current flowed out the strait in the southern part and came into Bohai Sea in the northern (not shown). The simulation captured main characteristics of tidal currents.

The changes in tidal energy act to influence tidal current as well. Four sites (where there was large human activity) were chosen to evaluate the changes caused by SLR (Figure 5b). It was clear to see that changes of tidal current was different in areas, in the Bohai Bay (site 8 and 9), influenced by sea level rise, tidal current speed was weakened, and there was a minor shift in time of maximum tidal current. In the Laizhou Bay (site 12) tidal current increased influenced by sea level-rise, and with SLR 3m scenario, tidal current could increased 5 cm/s, and in site 6 which located near Liaodong Bay, the effect of SLR on tidal current was small with little change in current speed.

DISCUSSION

Recently quick coastline changes caused by natural process and anthropogenic activity had influenced tidal system in the coastal zone (Huang *et al.*, 2015; Pelling *et al.*, 2013c; Wang *et al.*, 2014). Compared to coastline changes SLR is a relative slow and imperceptible process, however, the long-time affection of sea level rise can not only increase the risk of extreme water level but also influence tidal dynamic system. As coastline change was mainly induced by anthropogenic reclamation, recent coastline was kept unchanged for future projection when evaluating the affection induced by SLR. In the shallow water equation, sea level rise increased water depth, which led to intensify the propagation of waves and modify the reflected and incident waves. The tidal amplitude responds to SLR in a spatially non-uniform manner, with substantial amplitude decreases and increases in different SLR scenarios. To get details we choose four sites (marked in Figure 1a with 6, 8, 9 and 12, respectively) to compare the effects of different SLR scenario (Figure 6). Detailed examinations show that the amplitude of M_2 responded appropriately linearly to uniform SLR (Figure 6a), but was not proportional to SLR. Influenced by 0.5 m SLR, the maximum of increased (decreased) M_2 amplitude was 3 (8) cm, the maximum increment changed to 5 cm with 1m SLR, 11 cm with 2 m SLR scenario, and 15 cm under 3 m SLR condition. However, with the combination effects of water depth and bottom friction, the tidal energy dissipation (Figure 6b) showed a non-linear response to different increment of sea level, which is not consistent with amplitude changes.

The way of SLR implemented in the models could lead to qualitatively different results (Pelling *et al.*, 2013a; Pelling and Green, 2013; Ward *et al.*, 2012). Pickering *et al.* (2012) using a drying and flooding cell to study the effects of SLR with 2m and 10m on European shelf, found that the tidal amplitude effects was complex and non-linear to SLR. Most previous results used uniform SLR to study and predict its effects on coast in the future, neglected the spatial pattern of SLR in the domain. It was clearly to see that the effects of uniform SLR were much more different compared to effects of spatial pattern SLR (Figure 6a and b, marked with filled symbols). As Figure 1b showed, maximum rising trend of sea level was in Bohai Bay, from 5 mm/yr to 8 mm/yr, much larger than other areas of Bohai Sea. We assumed that the sea level trend keep constant, in the future after one hundred years the mean sea level in the Bohai Sea increased only 0.2 ~ 0.8 m and distributed spatially, simulation result showed that the effect was stronger than that of uniform SLR with 1 meter, even equivalent to effects of SLR with 2 meter, only considering amplitude changes (Figure 6a); and also in the migration of amphidromic points (Table 1), in the future the movement caused by spatial-distribution of SLR variation was farther than that caused by uniform SLR. Because tides in the Bohai Sea was forced by ocean tides from the Pacific, the wave frequency remains constant, as depth increased with the SLR the tidal wave propagates more quickly in the domain. With the spatial distribution of sea level-rise, tidal wave propagated into the Bohai Sea from adjoining sea, influenced by local changed depth, finally the accumulated results led to a complex and non-linear response to SLR (Figure 6c).

The changes caused by sea level-rise act to change tidal currents as well. As Figure 7a showed, there are three domains that residual currents changed dramatically, though maximum variance values are of the order of a few cm s^{-1}. The distribution of residual current change was similar to that of tidal energy change (not shown), which illustrated that the increment of tidal energy increased residual current. Compared Figure 7a and 7b, SLR with 1 meter mainly strengthened the effects caused by SLR 0.5 m, however, compared to the results between uniform SLR with 0.5m and spatial distrubiton-SLR after one hundred years (Figure 7a and 7c), the effects were intensified by spatial distribution of sea level rise, especially in Bohai Bay, where quicker rising rate of sea level increased local water level much more compared to other areas (Figure 1b), the local increased water depth would reduce incident waves and change reflected waves, which led to the increment of the residual current. Considering the spatial distribution of sea level variation, the influence of SLR was intenser than that of uniform variation. The migration of amphidromic points also showed the non-linear response between experiment case 0.5 and case100y (Table 1). As Zhou *et al.* (2015) confirmed that tidal current flow is indeed the main agent for transporting the fine sediment to the mud patch in the central South Yellow Sea, the changed tidal and residual currents caused by SLR were also related to the long-term transport of sediment in the Bohai Sea (Ji and Jiang, 1994; Li *et al.*, 2005; Wei *et al.*, 2004), for example near the Yellow River Delta weakened residual current may decrease the sediment transport outside and accumulate more sediment in the Delta. And in the Bohai Bay SLR decreased the residual currents, would increase the risk of port siltation.

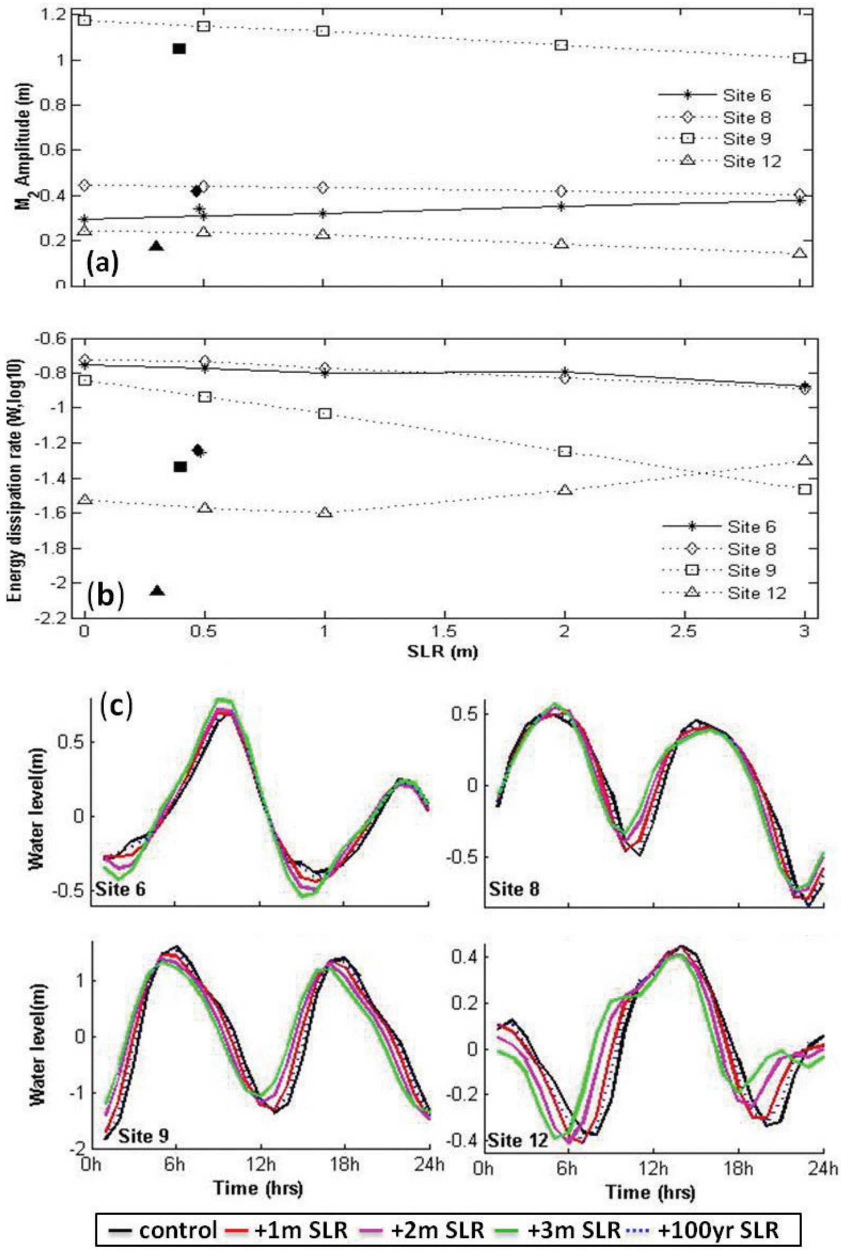

Figure 6. (a) M_2 amplitude response curves for station 6, 8, 9 and 12 (positions see Figure 1a); (b) The tidal energy dissipation at these four stations (shown as logarithmic values base on 10). The filled signals in the above two panels are values influenced by spatial distribution of SLR after one hundred years. (c) Water level curves (m) from different SLR scenario at 4 ports. The five sea level scenarios are shown 0 m (black line), 1 m (red line), 2 m (mauve line), 3 m (green line), and 100 years (blue dashed line)

CONCLUSION

The influence of sea level rise on tides in the Bohai Sea was assessed by a series of numerical experiments using ROMS model. The scenario of spatial distribution of SLR case was projected in the future keeping the present sea level rising trend derived from altimeter data after one hundred years, and the results were compared with other cases under different SLR conditions of uniform increment of water level from 0. 5 m to 3 m.

Table 1. *The location of amphidromic point of M_2 constituent under different SLR conditions*

Location	Case	SLR (m)	Latitude (°)	Longitude (°)
Yellow River Mouth	0	0	37.975	119.15
	0.5	0.5 m	37.95	119.25
	1	1m	37.95	119.30
	2	2 m	37.80	119.40
	3	3m	37.60	119.80
	100y	<0.8 m	37.75	119.55
Qinhuangdao	0	0	39.775	120.15
	0.5	0.5 m	39.7	120.1
	1	1m	39.625	120.08
	2	2 m	39.55	120
	3	3m	39.5	119.95
	100y	<0.8 m	39.6	120.05

Note: '0' is the control run, which represents the present tidal state in the Bohai Sea. The number means the value of uniform sea level rise. '100y' represents scenario after one hundred years with the present sea level rising rate.

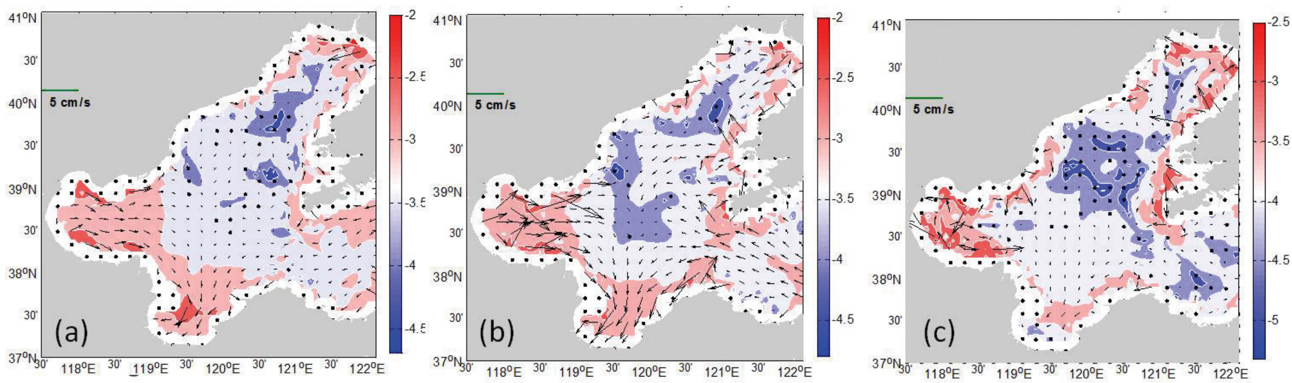

Figure 7. (a) Changes of tidal residual current between control run and uniform 0.5 m SLR run. (b) Changes of tidal residual current between control run and uniform 1 m SLR run. (c) Difference of effects from spatial distribution SLR run after one hundred years and uniform SLR 0.5 m. Values of both images are scaled by $\log_{10}$ with unit of m s^{-1}

The modeled results show that with synchronous increment of sea level, changes of M_2 amplitude responded to SLR non-proportionally, and showed a non-linear response. The M_2 amplitudes increased only around the two amphidromic points influenced by sea level rise. Due to the shape of coastline (headland etc.), changed bottom friction affected tidal energy flux and moved the amphidromic points to deep water under sea level rise conditions. Rising sea level increased water depth, combined local effect of sea level, it indeed reduced/increased tidal currents and residual currents, especially along coasts, which would change long-term sediment transport and influence the coastal erosion (Li *et al.*, 2005; Wei *et al.*, 2004). Simulated results showed that the response of tide regime was complex to spatial distribution of sea level rise and stronger than that from uniform rise of sea level, which illustrated the importance of considering spatial distribution of sea level rising when evaluating the risk of SLR in the future.

ACKNOWLEDGEMENTS

This study was supported by the Strategic Priority Research Program of the Chinese Academy of Sciences (grant no. XDA11020305) and the Key Deployment Project of Chinese Academy of Sciences (grant no. KZZD-EW-14). The altimeter products were produced by Ssalto/Duacs and distributed by Aviso, with support from Cnes (http://www.aviso.altimetry.fr/duacs/). We thank Dr. Jan Harff for encouragement and support.

LITERATURE CITED

Bao, X.; Gao, G., and Ju, Y., 2001. Three dimensional simulation of tide and tidal current characteristics in the *East China Sea*. *Oceanologica Acta*, 24 (2),135-149.

Chen, H.; Jiang, S., and Wang, F., 2011. Application of ADCIRC in M2 tide modeling in the Bohai Sea. *Chinese Marine Forcasts*, 28(4), 70-75. (in Chinese with English abstract)

Chu-Agor, M. L.; Munoz-Carpena, R.; Kiker, G.; Emanuelsson, A., and Linkov, I., 2011. Exploring vulnerability of coastal habitats to sea level rise through global sensitivity and uncertainty analyses. *Environmental Modeling & Software*, 26(5), 593-604.

Church, J. A. and White, N. J., 2006. A 20th century acceleration in global sea-level rise. *Geophysical Research Letters*, 33, L01602.

Church, J. A. and White, N. J., 2011. Sea-level rise from the late 19th to the early 21st century. *Surveys in Geophysics*, 32 (4), 585-602.

Cooper, J. A. G. and Pilkey, O. H., 2004. Sea-level rise and shoreline retreat: time to abandon the Bruun Rule. *Global and Planetary Change*, 43, 157-171.

Fang, G.; Wang, Y.; Wei, Z.; Choi, B. H.; Wang, X. and Wang, J., 2004. Empirical cotidal charts of the Bohai, Yellow, and East China Seas from 10 years of TOPEX/Poseidon altimetry. *Journal of Geophysical Research*, 109, C11006, doi: 10.1029/2004JC002484, 13pp.

Feng, G.; Jin, S., and Zhang, T., 2013. Coastal sea level changes in Europe from GPS, tide gauge, satellite altimetry and GRACE, 1993-2011. *Advances in Space Research*, 51(6), 1019-1029.

FitzGerald, D. M.; Fenster, M. S.; Argow, B. A., and Buynevich, I. V., 2008. Coastal impacts due to sea-level rise. *Annual Review of Earth and Planetary Sciences*, 36, 601-647.

Fu, L. L. and Cazenave, A. (Eds.), 2001. Satellite Altimetry and Earth Sciences: A Handbook of Techniques and Applications. *Academic Press*, *International Geophysics Series*.

Gong, Z.; Zhang, C.; Wan, L., and Zuo J., 2012. Tidal level response to sea-level rise in the yangtze estuary. *China Ocean Engineering*, 26(1), 109-122.

Greenberg, D. A., 1979. A numerical model investigation of tidal phenomena in the Bay of Fundy and Gulf of Maine. *Marine Geodesy*, 2(2),161-187.

Hao, Y.; Le, K. T., and Liu, X. Q., 2010. A numerical prediction of the tidal characteristics in 2010 of Yellow River Delta. *Chinese Marine Science*, 24(6), 43-46.

Haidvogel, D. B.; Arango, H. G.; Hedstrom, K.; Beckmann, A.; Malanotte-Rizzoli, P., and Shchepetkin, A. F., 2000. Model evaluation experiments in the North Atlantic Basin: Simulations in nonlinear terrain-following coordinates. *Dynamics of Atmospheres and Oceans*, 32, 239-281.

Hu, Z.; Guo, J.; Tan, Z., and Chang, X., 2014. Sea level variation in Hong Kong determined with Topex/Poseidon and tide gauge. *Journal of Geodesy and Geodynamics*, 34(4), 56,60.

Huang, J.; Xu, J.; Gao, S.; Lian, X., and Li, J., 2015. Analysis of influence on the Bohai Sea tidal system induced by coastline modification. *Journal of Coastal Research*, 73 (sp1), 359-363.

Ji, Z. and Jiang, Z., 1994. Impacts of sea level rise on coastal erosion in the Changjiang river delta and north Jiangsu coastal plain. *Chinese Geographical Science*, 4(4), 310-321.

Kang, S. K.; Foreman, M. G. G.; Lie, H. J.; Lee, J. H.; Cherniawsky, J., and Yum, K. D., 2002. Two-layer tidal modeling of the Yellow and East China Seas with application to seasonal variability of the M2 tide. *Journal of Geophysical Research*, 107(C3). doi:10.1029/2001JC000838.

Kuang, C. P.; Chen, W.; Gu, J.; Zhu, D. Z.; He, L. L., and Huang, H. C., 2014. Numerical Assessment of theImpacts of Potential Future Sea-Level Rise on Hydrodynamics of the Yangtze River Estuary, China. *Journal of Coastal Research*, 30(3), 586-597.

Leatherman, S. P.; Zhang, K., and Douglas, B. C., 2000. Sea-level rise shown to drive coastal erosion. EOS, 81(6), 55-57.

Lefèvre, F.; Le Provost, C., and Lyard, F. H., 2000. How can we improve a global ocean tide model at a regional scale? A test on the Yellow Sea and the East China Sea. *Journal of Geophysical Research*, 105(C4), 8707-8725.

Li, G. S.; Wang, H. L., and Li, B. L., 2005. A model study on seasonal spatial-temporal variability of the Lagrangian residual circulations in the Bohai Sea. *Journal of Geographical Sciences*, 15(3), 273-285.

Li, X.; Sun, X.; Wang, S.; Ye, F.; Li, Y., and Li, X., 2011. Characteristic analysis of Tianjin offshore tide. *Marine Science Bulletin*, 13, 40-49.

Lu, X. and Zhang, J., 2006. Numerical study on spatially varying bottom friction coefficient of a 2D tidal model with adjoint method. *Continental Shelf Research*, 26(16), 1905-1923.

Matsumoto, K.; Takashi T., and Masatsugu, O., 2000. Ocean tide models developed by assimilating Topex/Poseidon altimeter data into hydrodynamical model: A global model and a regional model around Japan. *Journal of Oceanography*, 56, 567-581.

Müller, M.; Arbic, B. K., and Mitrovica, J. X., 2011. Secular trends in ocean tides: Observations and model results. *Journal of Geophysical research*, 116, C05013, doi: 10.1029/2010JC006387.

Munk, W., 1997. Once again: once again-tidal friction. *Progress in Oceanography*, 40(1-4),7-35.

Pelling, H. E. and Green, J. A. M., 2013. Sea level rise and tidal power plants in the Gulf of Maine. *Journal of Geophysical Research Oceans*, 118, 2863-2873, doi: 10.1002/jgrc.20221.

Pelling, H. E.; Green, J. A. M., and Ward, S. L., 2013a. Modeling tides and sea level rise: to flood or not to flood. *Ocean Modeling*, 63, 21-29.

Pelling, H. E.; Uehara, K., and Green, J. A. M., 2013b. The impact of rapid coastline changes and sea level rise on the tides in the Bohai Sea, China. *Journal of Geophysical Research: Oceans*, 118(7), 3462-3472.

Pickering, M. D.; Wells, N. C.; Horsburgh, K. J., and Green, J. A. M., 2012. The impact of future sea-level rise on the European Shelf tides. *Continental Shelf Research*, 35, 1-15.

Poulos, S. E.; Ghionis, G., and Maroukian, H., 2009. The consequences of a futureecstatic sea-level rise on the deltaic coasts of Inner Thermaikos Gulf (Aegean Sea) and Kyparissiakos Gulf (Ionian Sea), Greece. *Geomorphology*, 107(1-2), 18-24.

Snoussi, M.; Ouchani, T.; Khouakhi, A., and Niang-Diop, I., 2009. Impacts of sea-level rise on the Moroccan coastal zone: Quantifying coastal erosion and flooding in the Tangier Bay. *Geomorphology*, 107(1-2), 32-40.

Song, D. H.; Wang, H. X.; Zhu, X. M., and Bao, X. W., 2013. Modeling studies of the far-field effects of tidal flat reclamation on tidal dynamics in the East China Seas. Estuarine, *Coastal and Shelf Science*, 133, 147-160.

SOAPRC (State Oceanic Administration People's Republic of China), 2009. Communiqué on Marine Environmental Quality of Bohai Sea 2008 (in Chinese). SOAPRC (State Oceanic Administration People's Republic of China).

Taylor, G. I., 1919. Tidal friction in the Irish Sea. Proc R Soc

London Ser A 96(678),330.

Valentim, J. M.; Vaz, L.; Vaz, N.; Silva, H.; Duarte, B.; Cacador, I., and Dias, J. M., 2013. Sea level rise impact in residual circulation in Tagus estuary and Ria de Aveiro lagoon. *Journal of Coastal Research*, 65, 1981–1986.

Wang, Y.; Wei, Z.; Fang, G.; Chen, H., and Gao, X., 2014. A numerical study on the effect of changes in water depth and coastline on M_2 tidal component near the Yellow River estuary. *Chinese Advances in Marine Science*, 32(2), 141–147. (in Chinese with English abstract)

Ward, S. L.; Green, J. A. M., and Pelling, H. E., 2012. Tides, sea-level rise and tidal power extraction on the European Shelf. *Ocean Dynamics*, 62, 1153–1167, doi: 10.1007/s10236-012-0552-6.

Warner, J. C.; Sherwood, C. R.; Signell, R. P.; Harris, C. K., and Arango, H. G., 2008. Development of a three-dimensional, regional, coupled wave, current, and sediment-transport model. *Computers & Geosciences*, 34, 284–1306.

Wei, H.; Hainbucher, D.; Pohlmann, T.; Feng, S. Z., and Suendermann, J., 2004. Tidal-induced Lagrangian and Eulerian mean circulation in the Bohai Sea. *Journal of Marine Systems*, 44(3–4), 141–151.

Wei, H.; Su, J.; Wan, R.; Wang, L. and Lin, Y., 2003. Tidal front and the convergence of anchovy (Engraulis japonicus) eggs in the Yellow Sea. *Fish Oceanography*, 12(45), 434–442.

Yao, Z.; He, R.; Bao, X.; Wu, D., and Song, J., 2012. M_2 tidal dynamics in Bohai and Yellow Seas: a hybrid data assimilative modeling study. *Ocean Dynamics*, 62(5), 753–769.

Yu, Y.; Yu, Y., and Zuo, J., 2003. Effect of sea level variation on tidal characteristic values for the East China Sea. *China Ocean Engineering*, 17, 369–382.

Yu, Y.; Liu, L., and Guo, M. K., 2007. Numerical research on tidal waves changes due to mean sea level rise in the Bohai Sea, the Huanghai Sea and the East China Sea II: Numerical modeling of tidal waves after mean sea level rise in the areas. *Periodical of Ocean University of China*, 37(1), 7–14. (in Chinese with English abstract)

Zhang, W.; Zhang, J.; Lin, R., and Zong, H., 2013. Tidal response of sea level rise in marginal seas near China. *Advance in water science*, 24, 243–250. (in Chinese with English abstract)

Zhou, C. Y.; Dong, P., and Li, G. X., 2015. Hydrodynamic processes and their impacts on the mud deposit in the Southern Yellow Sea. *Marine Geology*, 360, 1–16.

Zhu, X. and Liu, G., 2012. Numerical study on the tidal currents, tidal energy fluxes and dissipation in the Chinese Sea. *Oceanologia et Limnologia Sinica*, 43(3), 669–677. (in Chinese with English abstract)